Proceedings of the American Control Conference
Chicago, Illinois • June 2000

Elasto-Plastic Friction Model: Contact Compliance and Stiction

Pierre Dupont[1], Brian Armstrong[2], Vincent Hayward[3]
[1]Aerospace & Mechanical Engineering, Boston University
[2]Dept. Electrical Engineering and Computer Science, Univ.Wisc. - Milwaukee
[3]McGill Centre for Intelligent Machines, McGill University

March 17, 2000

Abstract

The presliding displacement and stiction properties of friction models are investigated. It is found that existing single-state-variable friction models possess *either* stiction or presliding displacement. Next, those models with continuous states are interpreted as examples of Prandlt's elasto-plastic material model. A class of general one-state models is derived that is stable, dissipative and exhibits *both* stiction and presliding displacement.

1 Introduction

The question of appropriate friction models has been raised many times; a survey cites 280 articles addressing issues of friction modeling, control and applications [2]. Some of the models most often used are the Coulomb+viscous friction model, and the Karnopp and LuGre models, which provide alternative tradeoffs amongst the desirable characteristics of a friction model. Here we show that existing models are unable torender both presliding displacement and stiction, and present an enhancement which is able to capture the advantages of existing models while providing a faithful rendering of stiction.

1.1 Friction Dynamics

Restricting attention to friction in machines (dominated by lubricated metal contacts) the frictional dynamics include Coulomb+viscous friction, static friction, the Stribeck velocity-friction curve, frictional memory and rising static friction [2].

1.1.1 Coulomb-Plus-Viscous Friction

The Coulomb+viscous friction model is commonly used because of its simplicity, and may be written:

$$f_f = f_C \, \mathrm{sgn}(v) + f_v \, v, \tag{1}$$

where f_f is the friction force, v the relative velocity of two bodies in contact, f_C the Coulomb friction level, and f_v the coefficient of dynamic friction. The model is not well suited for implementation because of the discontinuous sgn(·) function. The discontinuity can be addressed by modeling presliding displacement [4].

1.1.2 Presliding Displacement and Stiction

When a frictional contact is in static friction there may none the less be relative motion. This arises with tangential compliance and, because there is no true sliding, is called presliding displacement. A friction model renders presliding displacement if variations in applied force below the breakaway force produce elastic deformation and movement. A friction model renders static friction, or stiction, if, for applied forces smaller than a breakaway force, there is no *steady-state* relative motion.

Dahl introduced presliding displacement into friction modeling by incorporating tangential compliance [6]. The LuGre friction model [5] is an extension of Dahl's model, the LuGre model can represent: Coulomb+viscous friction, Stribeck friction curve, frictional memory, and rising static friction. The LuGre model may be written:

$$f_f = \sigma_0 \, z + \sigma_1 \, \dot{z} + \sigma_2 \, v, \quad \sigma_i > 0. \tag{2}$$

where z represents the state of strain in the frictional contact, and σ_0 and σ_2 are Coulomb and viscous friction parameters; and σ_1 provides damping for the tangential compliance. The signal $z(t)$ is governed by:

$$\dot{z} = v \left(1 - \frac{\sigma_0}{f_{ss}(v)} \, \mathrm{sgn}(v) \, z \right), \tag{3}$$

where $f_{ss}(v)$ represents the Stribeck curve, or steady-state friction-velocity curve.

Through presliding displacement, some motion is possible even when a mechanism is stuck in static friction [3], so a careful definition of static friction is required. A formal definition will be presented in section 2, here we informally consider that a friction model possesses a true stiction phase if there exists a breakaway force f_{ba} such that, for any friction force $f_f(t)$ that satisfies:

$$|f_f(t)| < f_{ba}, \; -\infty < t < t_1 \tag{4}$$

then all motions correspond to elastic deformation and are reversible. When the applied force is restored to

0-7803-5519-9/00 $10.00 © 2000 AACC

its initial value, the position comes, after a possible transient of presliding displacement, to its initial value.

As seen in Table 1, models in common use render several combinations of presliding displacement and stiction. The classic Coulomb friction model, like the Karnopp model, renders stiction but makes no reference to presliding displacement. Because of challenges posed by the discontinuity at zero velocity, the Coulomb friction model is sometimes regularized [12], leading to a model rendering neither presliding displacement nor stiction. The LuGre model renders presliding displacement but not stiction; and the Elasto-Plastic model, introduced here, renders both presliding displacement and stiction.

	Stiction	Presliding Displacement
Classic Coulomb and Karnopp Models	Yes	No
Regularized Coulomb	No	No
LuGre Model	No	Yes
Elasto-Plastic Model	Yes	Yes

Table 1: Comparison of four models of friction

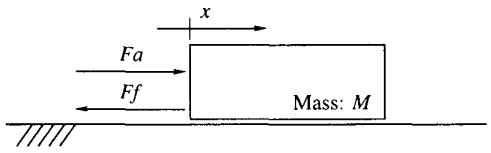

Figure 1: Simple mechanism simulated using four friction models.

To illustrate the four cases of presliding displacement and stiction, four simulations are presented in Figure 3. These simulations were the done with the simple mechanism illustrated in Figure 1 and with the applied force shown in Figure 2. The simulated models are:

1. Coulomb friction, regularized by smoothing the discontinuity at zero velocity (following [12]):

$$f_f = f_C \tanh(\frac{v}{v_0}) \tag{5}$$

with $m = 1.0$ [kg], $f_C = 1.0$ [N], and $v_0 = 0.01$ [m/s].

2. The Karnopp friction model [11], which introduces a band around $\dot{x} = 0$ where stiction is directly enforced by setting the velocity state to zero. $Dp = 0.01$ [m/s] (see [11] for details).

3. The LuGre friction model [5], given by Eqn's (2) and (3); with parameters $\sigma_0 = 100$, $\sigma_1 = 2.0$ and $\sigma_2 = 0$; and the Stribeck friction curve given by:

$$f_{ss}(v) = f_C + (f_{ba} - f_C)e^{-(v/v_s)^2} \tag{6}$$

where $f_{ba} = 1.1$ [N] is the breakaway force and $v_s = 0.1$ [m/s] is the characteristic velocity of the Stribeck curve [2].

4. The 'Elasto-Plastic' model, given by Eqn (2) and with $\dot{z}$ given by

$$\dot{z} = \dot{x}\left(1 - \alpha(z,\dot{x})\,\frac{\sigma_0}{f_{ss}(\dot{x})}\,\mathrm{sgn}(\dot{x})\,z\right)^i, \quad \frac{\sigma_0}{f_{ss}(\dot{x})} > 0,\ i \in \mathcal{Z} \tag{7}$$

where $\alpha(z,\dot{x})$ is used to achieve stiction. The $\alpha(z,\dot{x})$ used for these simulations is given by:

$$\alpha(z,\dot{x}) = \begin{cases} 0 & |z| < z_{ba} \\ \frac{1}{2}\sin\left(\pi\frac{z-\left(\frac{z_{max}+z_{ba}}{2}\right)}{z_{max}-z_{ba}}\right) + \frac{1}{2} & z_{ba} \le |z| < z_{max} \\ 1 & |z| \ge z_{max} \end{cases} \tag{8}$$

Requirements on the choice of $\alpha(z,\dot{x})$ are developed in Section 3.

The applied force of Figure 2 was chosen to challenge the stiction capability of each model, the force ramps up to cause break-away, and then returns to a level below that of Coulomb friction. Additionally, an oscillation is present, such as could be introduced by sensor noise or vibration.

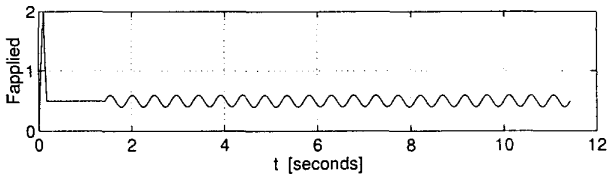

Figure 2: Applied force for the simulation of Figure 3

The response of friction models 1-4 is seen in Figure 3 and summarized in Table 1. Model 1 renders neither presliding displacement nor stiction. The absence of stiction is seen in the time interval from 2-10 seconds where steady drift occurs.

Model 2, the Karnopp model, renders stiction but no presliding displacement: during the interval from 2-10 seconds there is no motion.

Model 3, the LuGre model [5], renders presliding displacement, in the form of the oscillatory response to the oscillatory applied force, but does not render stiction. Rather, there is a steady drift in position during the interval from 2-10 seconds.

Model 4, the Elasto-Plastic model, renders both presliding displacement and stiction. Presliding displacement is seen in the oscillatory response to the oscillatory applied force, and stiction is indicated by the absence of net motion during the interval from 2-10 seconds. Model 4 shows the importance of a careful definition of stiction:

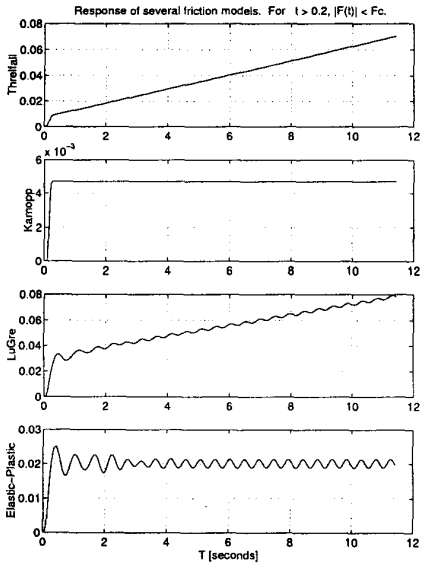

Figure 3: Response of four friction models to the applied force of Figure 2.

when time-varying forces are applied, even if $F_{applied}$ is less than the break-away force, presliding displacement gives rise to motion.

1.1.3 Additional Frictional Dynamics

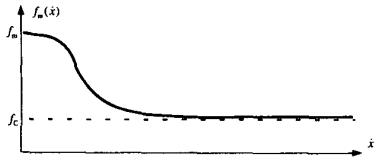

Figure 4: Stribeck curve of steady-state friction force versus rigid body velocity $\dot{x}$. f_m and f_C correspond to the maximum steady-state and Coulomb magnitudes of friction force, respectively.

The Stribeck curve describes friction as a function of *steady-state* sliding velocity. A typical example is seen in figure 4. Individual consideration of Stribeck friction, frictional memory and rising static friction is not the focus of this paper. As with the LuGre model, Stribeck friction, frictional memory and rising static friction are rendered by the Elasto-Plastic friction model.

2 Internal State Models

Consider the class of friction models involving a single state variable in which rigid body displacement x is decomposed into its elastic and plastic (inelastic) components z and w:

$$x = z + w. \tag{9}$$

Such "elasto-plastic" models were proposed by Prandlt to represent the behavior of solids under stress [13], are applied here to represent friction. Referring to Dahl's model [6] to Eqn's (3) or (7), it is observed that distributing $\dot{x}$ and integrating any of these equations over an interval of time yields the form of Eqn (9).

The state variable z is taken to be the elastic (memoryless) portion of the displacement while the implicit variable w describes the plastic (history dependent) portion of the displacement. It can be represented by the physical analogy depicted in Figure 5. Here, the mass experiences a friction force due to the deformation (and inherent damping) of a single lumped asperity contact. The state or motion history for this class of models is completely embodied in the variable z. The system input is rigid body velocity $\dot{x}$ and its output is friction force f_f.

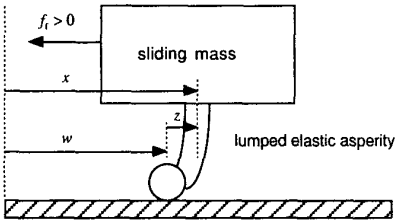

Figure 5: Model of block subject to friction force showing decomposition of displacement x into elastic and inelastic components, z and w.

It should be noted that while the depicted system is only a physical analogy, the decomposition of total tangential displacement into elastic and plastic components is completely general. In the following subsections we define stiction, passivity and other properties in terms of this decomposition. Many existing state variable models fit within this framework including the Haessig and Friedland, Dahl and LuGre models [6, 8, 5].

2.1 Stiction

Stiction corresponds to the existence of a breakaway displacement $z_{\text{ba}} > 0$ such that for $|z| \leq z_{\text{ba}}$ all motion of the friction interface consists entirely of elastic displacements. In this context, elastic displacement z corresponds to presliding displacement and plastic (inelastic) displacement w corresponds to sliding displacement. Thus, stiction can be defined formally in terms of plastic displacement w as follows.

Definition 1 *A friction model possesses a true stiction phase if there exists a breakaway displacement* $z_{\text{ba}} > 0$ *such that* $|z(t)| \leq z_{\text{ba}}$ *implies* $\dot{w}(t) = 0, \forall \dot{x} \in \mathcal{R}$.

In solid mechanics, the stiction condition is analogous to the existence of an elastic region on a material's stress-strain curve. The breakaway displacement can be related to the strain experienced at the elastic limit, the stress at which plastic yielding begins to occur [10].

2.2 Sticking and Sliding

Sticking and sliding can now be defined in terms of rate equations which follow directly from the definition of the state variable z.

$$\left.\begin{array}{rcl} \dot{x} &=& \dot{z} \\ \dot{w} &=& 0 \end{array}\right\} \text{ sticking—elastic displacement,}$$
$$\left.\begin{array}{rcl} \dot{x} &=& \dot{w} \\ \dot{z} &=& 0 \end{array}\right\} \text{ sliding—plastic displacement.} \tag{10}$$

Combined sticking and sliding require a more careful description because there are actually three cases involved. The governing rate equation, from (9), is given by:

$$\dot{x} = \dot{z} + \dot{w} \tag{11}$$

Case 1: Transitions between sticking and sliding. Here we have

$$\text{sgn}(\dot{x}) = \text{sgn}(\dot{w}) = \text{sgn}(\dot{z}). \tag{12}$$

During the transition from sticking to sliding, the collection of asperity contacts begins to deform plastically and shear. They do not shear all at once, however; there is some finite displacement over which both the presliding and slip rates are nonzero. The signed equalities constrain the rates of elastic and plastic deformation to fall between the limits obtained in the cases of pure sticking and steady-state sliding.

Case 2: Elastic relaxation due to the Stribeck effect.

The Stribeck curve, as depicted in Figure 4, indicates that the steady-state friction force is a decreasing function of velocity magnitude. Following an increase in velocity, the elastic deformation must decrease, despite continued sliding, to produce the smaller steady-state friction force. The inequality

$$\text{sgn}(\dot{x}) \neq \text{sgn}(\dot{z}). \tag{13}$$

will hold during the elastic relaxation.

If the friction model includes an elastic damping term, such as $\sigma_1 \dot{z}$ in Eqn (2), the elastic damping can reverse the direction of the friction force during relaxation—rendering the model nondissipative [1]. This is seen in figure 6. We call this the 'Stribeck slingshot effect' because the modeled friction actually accelerates the mass forward, which, of course, is a non-physical modeling artifact. The Stribeck slingshot effect can be avoided by proper choice of model parameters (see Eqn (19), below and [1]).

Case 3: Elastic 'super relaxation' following motion reversal. Immediately following a reversal of velocity $\dot{x}$, the magnitude of the elastic deformation decreases. In the context of Figure 5, the elastic asperity must relax before stretching in the opposite direction.

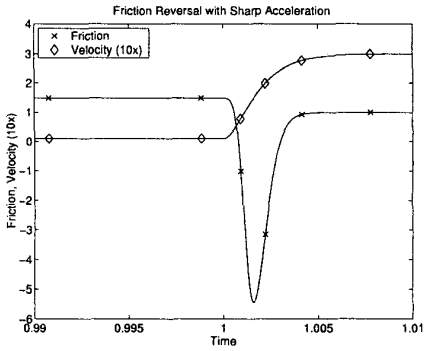

Figure 6: Friction reversal arising with an internal state friction model and Stribeck friction; LuGre model, system of figure 1 with parameters $M = 1$, $f_C = 1$, $f_{ba} = 1.5$, $\sigma_0 = 10000$, $\sigma_1 = 200$, $\sigma_2 = 0$, $v_s = 0.1$.

In friction models, the rate of relaxation may exceed the rigid body velocity, giving

$$\text{sgn}(\dot{x}) \neq \text{sgn}(\dot{w}). \tag{14}$$

We refer to this phenomenon as super relaxation.

Super relaxation appears to be a non-physical condition for an inertialess contact model. Its consequence is that during relaxation some elastic energy that otherwise would be returned to the sliding mass is dissipated through sliding. See [7] for further details.

2.3 State variable models in the literature

The equations describing the dynamics of the frictional state variable, (7), and the friction force, (2), are repeated here for convenience.

$$\dot{z} = \dot{x}\left(1 - \alpha(z,\dot{x})\,\frac{\sigma_0}{f_{ss}(\dot{x})}\,\text{sgn}(\dot{x})\,z\right)^i, \quad \frac{\sigma_0}{f_{ss}(\dot{x})} > 0,\ i \in \mathcal{Z} \tag{15}$$

$$f_f = \sigma_0\, z + \sigma_1\, \dot{z} + \sigma_2\, \dot{x}, \quad \sigma_i > 0. \tag{16}$$

By the proper choice of model parameters σ_i and function α, these equations encompass a number of friction models including those of Dahl [6], Haessig and Friedland [8] and Canudas de Wit *et al.* [5]. In particular, the following theorem states the conditions under which a model of this form can exhibit stiction.

Theorem 1 *A friction model described by (15)-(16) possesses a stiction phase if and only if there exists a* $z_{ba} > 0$ *such that* $\alpha(z,\dot{x}) = 0$, $\forall z \in \{|z| \leq z_{ba}\}, \forall \dot{x} \in \mathcal{R}$. *This result is independent of the integer exponent used in Dahl's model.*

Proof: Assume that the model possesses a stiction phase and is sticking with $\dot{z} = \dot{x}$. By (15) we must have: $\alpha(z,\dot{x})\,\text{sgn}(\dot{x})\,[\sigma_0/f_{ss}(\dot{x})] \equiv 0$. Since $\sigma_0/f_{ss}(\dot{x}) > 0$, this is true if either $z(t) \equiv 0$ or

$\alpha(z,\dot{x}) \equiv 0$. But $z(t) \equiv 0$ contradicts the assumed existence of a stiction phase. Thus, it must be true that $\alpha(z,\dot{x}) = 0, \forall z \in \{|z| \leq z_{\rm ba}\}, \forall \dot{x} \in \mathcal{R}$.

Now assume that $\alpha(z,\dot{x}) = 0, \forall z \in \{|z| \leq z_{\rm ba}\}, \forall \dot{x} \in \mathcal{R}$. Clearly $\dot{z} = \dot{x}$ and $\dot{w} = 0$ for $|z| \leq z_{\rm ba}$ so that the model possesses a stiction phase.

These results can be used to evaluate the properties of models fitting the form of (15)-(16). For example, the LuGre model satisfies the inequality

$$0 < \alpha(z,\dot{x}) \frac{\sigma_0}{f_{\rm ss}(\dot{x})} < \infty \tag{17}$$

By the preceding theorem, we see that Dahl-like models such as the LuGre model do not possess a stiction phase. Thus, with the exception of a constant friction force, $f_{\rm f}(t) = f_{\rm f}(t_0), \forall t \geq t_0$, any friction force history produces slip.

3 The Elasto-Plastic Model

In this section, we present a model of the form of (15)-(16) that possesses the following properties:

1. The presliding displacement is bounded: If $|z(0)| \leq z_{\rm m}$ with $z_{\rm m} = f_{\rm m}/\sigma_0 > 0$ then $|z(t)| \leq z_{\rm m}, \forall t \geq 0$.
2. Super relaxation is precluded: $0 \leq dz/dx \leq 1$ if no Stribeck effect is modeled and $-\infty < dz/dx \leq 1$ otherwise.
3. The model possesses a stiction phase: A breakaway displacement $z_{\rm ba} > 0$ exists such that the model behaves elastically for $|z| < z_{\rm ba}$.
4. During sliding, the friction force opposes slip: $\mathrm{sgn}(f_{\rm f}) = \mathrm{sgn}(\dot{w}), \forall \dot{w} \neq 0$.
5. The model is dissipative for all $\dot{x} \neq 0$.

To achieve these properties, we define the piecewise continuous function $\alpha(z,\dot{x})$ as follows with
When $\mathrm{sgn}\,(\dot{x}) = \mathrm{sgn}\,(z)$:

$$\alpha\,(z,\dot{x}) = \begin{cases} 0 & |z| \leq z_{\rm ba} \\ 0 < \alpha < 1 & z_{\rm ba} < |z| < z_{\max}\,(\dot{x}) \\ 1 & |z| \geq z_{\max}\,(\dot{x}) \end{cases} \tag{18}$$

$$0 < z_{\rm ba} < z_{\max}(\dot{x}) = \frac{f_{\rm ss}(\dot{x})}{\sigma_0}, \forall \dot{x} \in \mathcal{R} \tag{19}$$

When $\mathrm{sgn}\,(\dot{x}) \neq \mathrm{sgn}\,(z)$:

$$\alpha\,(z,\dot{x}) = 0$$

Graphically, the function $\alpha(z,\dot{x})$ for $\mathrm{sgn}(\dot{x}) = \mathrm{sgn}(z)$, has the general shape depicted in Figure 7. This function controls the rate of change of z with respect to x, as is apparent from Eqn (15).

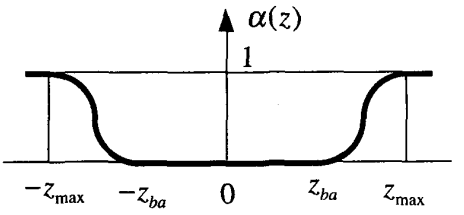

Figure 7: Plot of $\alpha(z,\dot{x})$ for $\mathrm{sgn}(\dot{x}) = \mathrm{sgn}(z)$.

We now prove that the model described by Eqn's (15)-(16) and (18)-(19) possesses properties 1-5.

Proof of Property 1, Presliding Displacement is Bounded: Following Canudas de Wit *et al.* [5], define the positive definite Lyapunov function $V = z^2/2$ and evaluate its time derivative using (15) and (18):

$$\begin{aligned} \frac{dV}{dt} &= z\left[\dot{x}\left(1 - \alpha(z,\dot{x})\tfrac{\sigma_0}{f_{\rm ss}(\dot{x})}\,\mathrm{sgn}(\dot{x})\,z\right)\right] \\ &= -|z||\dot{x}|\left(\alpha(z,\dot{x})\tfrac{\sigma_0}{f_{\rm ss}(\dot{x})}|z| - \mathrm{sgn}(\dot{x})\;\mathrm{sgn}(z)\right) \end{aligned} \tag{20}$$

For $|z| > f_{\rm m}/\sigma_0 \geq f_{\rm ss}(\dot{x})/\sigma_0\alpha(z,\dot{x})$, the derivative is negative. Thus we can conclude that the set $\Omega = \{z : |z| \leq f_{\rm m}/\sigma_0\}$ is invariant with respect to (15), (18) and (19). All solutions $z(t)$ starting in Ω remain there. In the absence of the Stribeck dependency, $f_{\rm ss}(\dot{x}) = f_{\rm C}$, a constant.

Proof of Property 2, Conditions for sticking and sliding are satisfied: By Eqn (7) this property is equivalent to, with no Stribeck effect:

$$0 \;\leq\; \alpha(z,\dot{x})\frac{\sigma_0}{f_{\rm ss}(\dot{x})}\;\mathrm{sgn}(\dot{x}) \leq 1 \tag{21}$$

And with Stribeck effect:

$$0 \;\leq\; \alpha(z,\dot{x})\frac{\sigma_0}{f_{\rm ss}(\dot{x})}\;\mathrm{sgn}(\dot{x})\;z < f_{\rm m}/f_{\rm C} < \infty \tag{22}$$

The lower bound follows directly from (18). The upper bound follows from Property 1, equations (18) and (19), and Figure 4.

Proof of Property 3, Existence of a Stiction phase: The existence of a stiction phase follows directly from (18) and Theorem 1.

Proof of Property 4, Friction opposes slip: We will present the case when a Stribeck effect is not present. The additional conditions needed when to assure Property 4 when Stribeck friction is present are addressed in [1]. In either case, we have $\mathrm{sgn}(\dot{x}) = \mathrm{sgn}(\dot{w})$ from Property 2 and (12). We can therefore attempt to prove

$$\mathrm{sgn}(f_{\rm f} = \sigma_0\,z + \sigma_1\,\dot{z} + \sigma_2\,\dot{x}) = \mathrm{sgn}(\dot{x}), \forall \dot{w} \neq 0. \tag{23}$$

Substituting (18) we obtain

$$\operatorname{sgn}\left[\sigma_0\, z + \sigma_1\, \dot{x}\left(1 - \alpha(z,\dot{x})\,\frac{\sigma_0}{f_C}\,\operatorname{sgn}(\dot{x})\, z\right) + \sigma_2\, \dot{x}\right] = \operatorname{sgn}(\dot{x}), \forall \dot{w} \neq 0. \quad (24)$$

By the inequality (21), it is clear that each term will individually satisfy the equation if $\operatorname{sgn}(z) = \operatorname{sgn}(\dot{x})$. But if $\operatorname{sgn}(z) \neq \operatorname{sgn}(\dot{x})$ then by (15)-(16), $\dot{z} = \dot{x}$ and the system is sticking: $\dot{w} = 0$.

Proof of Property 5, The model is dissipative: For dissipativity, we will consider the map $\dot{x} \mapsto f_f$, from rigid body velocity to friction force. Using $V(t) = 1/2\sigma_0 z^2$ as a positive definite storage function, we write the input-output product as

$$\begin{aligned} \dot{x} f_f &= (\dot{z} + \dot{w})(\sigma_0\, z + \sigma_1\, \dot{z}) + \sigma_2\, \dot{x}^2 \\ &= \dot{V} + \sigma_1\, \dot{z}^2 + \dot{w}\, f_f + \sigma_2\, \dot{x}^2 \\ &> \dot{V}, \quad \forall \dot{x} \neq 0. \end{aligned} \quad (25)$$

We can conclude that the map $\dot{x} \mapsto f_f$ is dissipative for any nonzero input. Note that each term in (25) has the units of power. During sticking, the energy dissipation rate is $\sigma_1 \dot{x}^2$, owing to asperity damping. During sliding, Property 4 assures us a positive rate of dissipation, $\dot{w} f_f$.

4 Demonstrations of the Elasto-Plastic Model

Like the LuGre model the Elasto-Plastic model will qualitatively render Stribeck friction, frictional memory, rising static friction, in addition to presliding displacement. Additionally, stiction is rendered. Modeling of presliding displacement and stiction are shown in figure 3. Modeling of frictional memory is demonstrated in figure 8. This figure was generated with the motion and model parameters used by Canudas *et al.* [5] to illustrate the ability of the state-variable friction model to render to the frictional memory demonstrated experimentally by Hess and Soom [9].

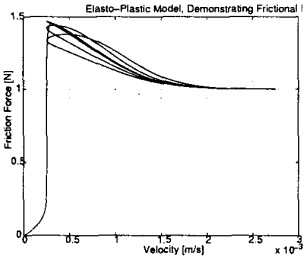

Figure 8: Friction during oscillatory motions at 3 frequencies, frictional memory gives rise to the differing levels of friction for acceleration and deceleration.

5 Conclusions

The state-variable friction models are desirable for many applications because they avoid switch functions or discontinuities. It has been seen, however, that modeling presliding displacement and sliding in a single function gives rise to subtle issues. These issues have been explored, and an innovation is introduced which offers the advantages of a state-variable friction model, and renders both presliding displacement and static friction.

References

[1] Friedhelm Altpeter. *Friction Modeling, Identification and Compensation.* PhD thesis, Ecole Polytechnique Federale de Lausanne, 1999.

[2] B. Armstrong-Hélouvry, P. Dupont, and C. Canudas de Wit. A survey of models, analysis tools and compensation methods for the control of machines with friction. *Automatica*, 30(7):1083–1138, 1994.

[3] Brian Armstrong-Helouvry. *Control of Machines with Friction.* Norwell Massachusetts: Kluwer Academic Publishers, 1991.

[4] P.A. Bliman and M. Sorine. A system-theoretic approach of systems with hysteresis. application to friction modelling and compensation. In *European Control Conference, ECC'93*, volume 4, pages 1844–45. Groningen, The Netherlands, 1993.

[5] C. Canudas de Wit, H. Olsson, K.J. Aström, and P. Lischinsky. A new model for control of systems with friction. *IEEE Trans. on Automatic Control*, 40(3):419–425, 1995.

[6] P.R. Dahl. Solid friction damping of mechanical vibrations. *AIAA J.*, 14(12):1675–82, 1976.

[7] Pierre Dupont, Vincent Hayward, and Brian Armstrong. Single state elasto-plastic models for friction compensation. *IEEE Trans. on Automatic Control*, 2000. Under Review.

[8] D.A. Haessig and B. Friedland. On the modeling and simulation of friction. *J. of Dynamic Systems, Measurement and Control*, 113(3):354–362, 1991.

[9] D. P. Hess and A. Soom. Friction at a lubricated line contact operating at oscillating sliding velocities. *J. of Tribology*, 112(1):147–52, 1990.

[10] Gere J. and Timoshenko S. *Mechanics of Materials.* PWS Publishing Co., 1997.

[11] D. Karnopp. Computer simulation of stick-slip friction in mechanical dynamic systems. *ASME J. of Dynamic Systems, Measurement and Control*, 107(1):100–103, 1985.

[12] D.C. Threlfall. The inclusion of coulomb friction in mechanisms programs with particular reference to dram. *Mechanism and Machine Theory*, 13(4):475–83, 1978.

[13] A. Visitin. *Differential Models of Hysteresis.* Springer-Verlag: Berlin, Heidelberg, 1994.